OPEN ACCESS

Original research

Lactobacillus gallinarum modulates the gut microbiota and produces anti-cancer metabolites to protect against colorectal tumourigenesis

Naoki Sugimura,[1,2] Qing Li,[1,3] Eagle Siu Hong Chu,[1] Harry Cheuk Hay Lau ,[1] Winnie Fong,[1] Weixin Liu,[1] Cong Liang,[4] Geicho Nakatsu,[5] Anthony Chin Yang Su,[1] Olabisi Oluwabukola Coker,[1] William Ka Kei Wu ,[3] Francis Ka Leung Chan ,[1] Jun Yu [1]

► Additional supplemental material is published online only. To view, please visit the journal online (http://dx.doi.org/10.1136/gutjnl-2020-323951).

For numbered affiliations see end of article.

Correspondence to
Dr Jun Yu, Medicine and Therapeutics, The Chinese University of Hong Kong, Hong Kong, Hong Kong; junyu@cuhk.edu.hk
Professor Francis Ka Leung Chan; fklchan@cuhk.edu.hk

NS and QL are joint first authors.

Received 22 December 2020
Accepted 7 December 2021
Published Online First 22 December 2021

Watch Video
gut.bmj.com

To cite: Sugimura N, Li Q, Chu ESH, *et al*. *Gut* 2022;**71**:2011–2021.

ABSTRACT

Objective Using faecal shotgun metagenomic sequencing, we identified the depletion of *Lactobacillus gallinarum* in patients with colorectal cancer (CRC). We aimed to determine the potential antitumourigenic role of *L. gallinarum* in colorectal tumourigenesis.

Design The tumor-suppressive effect of *L. gallinarum* was assessed in murine models of CRC. CRC cell lines and organoids derived from patients with CRC were cultured with *L. gallinarum* or *Escherichia coli* MG1655 culture-supernatant to evaluate cell proliferation, apoptosis and cell cycle distribution. Gut microbiota was assessed by 16S ribosomal DNA sequencing. Antitumour molecule produced from *L. gallinarum* was identified by liquid chromatography mass spectrometry (LC-MS/MS) and targeted mass spectrometry.

Results *L. gallinarum* significantly reduced intestinal tumour number and size compared with *E. coli* MG1655 and phosphate-buffered saline in both male and female murine intestinal tumourigenesis models. Faecal microbial profiling revealed enrichment of probiotics and depletion of pathogenic bacteria in *L. gallinarum*-treated mice. Culturing CRC cells with *L. gallinarum* culture-supernatant (5%, 10% and 20%) concentration-dependently suppressed cell proliferation and colony formation. *L. gallinarum* culture-supernatant significantly promoted apoptosis in CRC cells and patient-derived CRC organoids, but not in normal colon epithelial cells. Only *L. gallinarum* culture-supernatant with fraction size <3 kDa suppressed proliferation in CRC cells. Using LC-MS/MS, enrichments of indole-3-lactic acid (ILA) was identified in both *L. gallinarum* culture-supernatant and the gut of *L. gallinarum*-treated mice. ILA displayed anti-CRC growth *in vitro* and inhibited intestinal tumourigenesis *in vivo*.

Conclusion *L. gallinarum* protects against intestinal tumourigenesis by producing protective metabolites that can promote apoptosis of CRC cells.

Significance of this study

What is already known on this subject?

⇒ *Lactobacillus gallinarum* is one of the most depleted probiotic species in the stool of patients with colorectal cancer (CRC).

What are the new findings?

⇒ Administration of *L. gallinarum* inhibited colorectal tumourigenesis in *Apc*$^{Min/+}$ mice and in azoxymethane/dextran sulfate sodium-treated mice.

⇒ *L. gallinarum* increased abundances of gut probiotics and depleted potential gut pathogens.

⇒ *L. gallinarum* culture-supernatant suppressed cell proliferation, and induced apoptosis in CRC cell lines and in organoids derived from patients with CRC.

⇒ Secreted non-protein molecule(s) with a molecular weight <3 kDa from *L. gallinarum* mediated the anti-CRC effect.

⇒ Indole-3-lactic acid, a small molecule with known anti-inflammatory property, was identified as the most enriched metabolite produced by *L. gallinarum*.

How might it impact on clinical practice in the foreseeable future?

⇒ The probiotic *L. gallinarum* is a potential prophylactic for preventing CRC in humans.

INTRODUCTION

Colorectal cancer (CRC) is the third most commonly diagnosed malignancy and the second leading cause of cancer death in the world.[1] There are many risk factors associated with CRC carcinogenesis including genetic alterations, lifestyle and environmental factors.[2] Over the last decade, gut microbiota has been shown to play a key role in CRC development. Certain probiotic bacteria such as *Streptococcus thermophilus* and *Lactobacillus rhamnosus* have demonstrated anticarcinogenic properties.[3 4]

Most *Lactobacillus* species are classified as lactic acid bacteria (LAB). LAB are generally found in fermented food, such as decomposing plants and milk products, and they are widely accepted to be used as probiotics for humans.[5] The beneficial effects of LAB for diseases have been reported extensively[6 7] and preclinical studies have shown its abilities to reduce chronic inflammation associated with

cancer development.[8 9] Using shotgun metagenomic sequencing, we identified a probiotic species *Lactobacillus gallinarum* being significantly depleted in the stool of patients with CRC,[10] suggesting that it might play a role in suppressing CRC. In this study, we showed that *L. gallinarum* could abrogate colorectal tumourigenesis in mouse models, human CRC-derived organoids and CRC cell lines through promoting apoptosis. This tumour-suppressing effect was attributed to indole-3-lactic acid (ILA), a metabolite generated by *L. gallinarum*.

MATERIALS AND METHODS

Animal experiments

Male and female $Apc^{Min/+}$ C57B/6 mice, which can faithfully recapitulate the human familial adenomatous polyposis, was used as a mouse model of spontaneous CRC.[11] $Apc^{Min/+}$ mice at 5–6 weeks old were divided into three groups with or without CH-223191 treatment: (1) phosphate-buffered saline (PBS); (2) *Escherichia coli* MG1655 and (3) *L. gallinarum*. *Lactobacillus casei* was further used as a LAB control. *L. gallinarium* was cultured in MRS broth (Difco Laboratories, Detroit, Minnesota, USA) and *L. casei* and *E. coli* MG1655 were cultured in brain heart infusion (BHI) broth. After 1 day, each of the bacteria was collected and resuspended in PBS and then gavaged to mice (1×10^8 colony-forming unit (CFU)/100 μL PBS per mouse). Male and female mice were gavaged once daily for 8 and 12 weeks, respectively, for the development of neoplastic lesions. Body weight and stool were examined weekly.

The azoxymethane (AOM)/dextran sulfate sodium (DSS) model, which can mimic human colitis-associated carcinoma (CAC), was also established. Male and female C57BL/6 mice at 6 weeks old were intraperitoneally injected with a single dose of 10 mg/kg AOM (Merck, Darmstadt, Germany), followed by 2% DSS (MP Biomedicals, Solon, Ohio, USA) administration for 1 week. AOM/DSS-induced CRC mice were gavaged with *L. gallinarium* and *E. coli* MG1655 suspension following the same schedule.

Mouse colonoscopy (Karl Storz Endoskope, Tuttlingen, Germany) was performed prior to sacrifice. The colonoscope was inserted into anus and advanced proximally under direct visualisation, facilitated by air insufflation, and representative pictures of the colon tumour from each group were recorded. After neoplastic lesions developed, mice were anaesthetised and sacrificed. Small intestines and colons of mice were longitudinally opened and rinsed with PBS. Total number of tumours in small intestine and colon were recorded. Size of each tumour was measured using previous published formula.[12]

16S rDNA gene sequence analysis

Raw de-multiplexed FASTQ files were preprocessed in Mothur.[13] Contigs were created using Needleman-Wunsch alignment algorithm with default parameters,[14] and aligned against the SILVA database (V.123) using NAST algorithm.[15 16] We removed any contigs with homopolymers of >8 nucleotides and retained all that mapped within the identical coordinates. Any sequence pairs with mismatch difference of ≤2 were preclustered to reduce amplicon sequencing noises. Chimeric sequences were culled using de novo UChime.[17] Postquality controlled sequences were classified using Greengenes 16S rRNA database (V.13.8). We discarded any sequences of eukaryotic, archaea, mitochondrial, chloroplastic or unknown origins before binning them into operational taxonomic units (OTUs) at 97% identity threshold. The lowest taxonomic annotation for an OTU was defined as having a consensus assignment score of ≥80. Sequence count table was rarefied to the smallest number of reads per sample (ie, 44 845 reads) to reduce the effects of variable sequencing depths on downstream analyses. The significance of Alpha diversity was assessed by Wilcoxon rank-sum test. Beta diversity was visualised by principal coordinate analysis. P value <0.05 was considered statistically significant. Differential abundance analysis was performed with one-way analysis of variance (ANOVA). Average fold change for each OTU and heatmap was computed in the R Project for Statistical Computing.[18] The p values obtained were adjusted for multiple comparisons by the false discovery rate method. The corresponding q<0.05 was considered statistically significant.

Bacterial strains and culture conditions

L. gallinarum (ATCC 33199) and *L. casei* (ATCC BAA-2843) were purchased from American Type Culture Collection (ATCC; Manassas, Virginia, USA). *E. coli* strain MG1655 (ATCC 700926), a non-pathogenic human commensal intestinal bacterium, was included as a negative control.[19] They were cultured in MRS broth or BHI broth as appropriate at 37°C under aerobic condition.

CRC patient-derived organoid culture

CRC organoids derived from 2 patients (74 and 816) were obtained from Princess Margaret Living Biobank (Toronto, Ontario, Canada), and embedded into Matrigel (Corning, Corning, New York, USA). Culture medium was changed every 2 days. After 5 days of culture, Matrigel was removed to expose organoids by mechanical stress and/or TrypLE digestion (Sigma-Aldrich). Organoids were then collected for further experiments. The detailed information about these two patients with CRC is listed in online supplemental table 1.

Cell viability assay

Cell viability was measured by 3-(4,5-dimethylthiazoly-2-yl)-2,5-diphenyltetrazolium bromide (MTT) (Sigma-Aldrich) assay. Cells were seeded on 96-well plates at 1.0×10^3 cells per well and incubated for 24 hours before treatment. Cells were cultured in Dulbecco's Modified Eagle's Medium with addition of bacterial supernatants at different concentrations (5%, 10% or 20%) or the same amount of ILA (Sigma-Aldrich) comparable to that of 20% *L. gallinarum* culture supernatant (LGCS). Cell proliferation was measured by MTT assay for five consecutive days. The amount of MTT formazan product was determined by measuring absorbance at a wavelength of 570 nm (OD_{570}) with a microplate reader (Multiskan GO Microplate Spectrophotometer, Thermo Scientific, Vantaa, Finland). For pharmacological inhibition of aryl hydrocarbon receptor (AhR), CH-223191 (100 nM) was added 12 hours before the treatment with bacteria culture supernatant.

Apoptosis assay and cell cycle analysis

Cells were plated on 6-well plates 24 hours prior to treatment, and cultured in medium containing 10% LGCS, *E. coli* culture supernatant (ECCS) or BHI. CRC patient-derived organoids were cultured on 6-well plates, and 10% LGCS, ECCS or BHI was added to Matrigel and growth medium. After 5 days of treatment, cells and organoids were digested in 0.25% trypsin-EDTA (Gibco-Invitrogen, Grand Island, New York, USA) and TrypLE, respectively. For apoptosis assay, the proportion of apoptotic cells was evaluated by dual staining with Annexin V-PE and 7-aminoactinomycin D (7-AAD) (BD Pharmingen, San Jose, California, USA). Combination of Annexin V-PE and

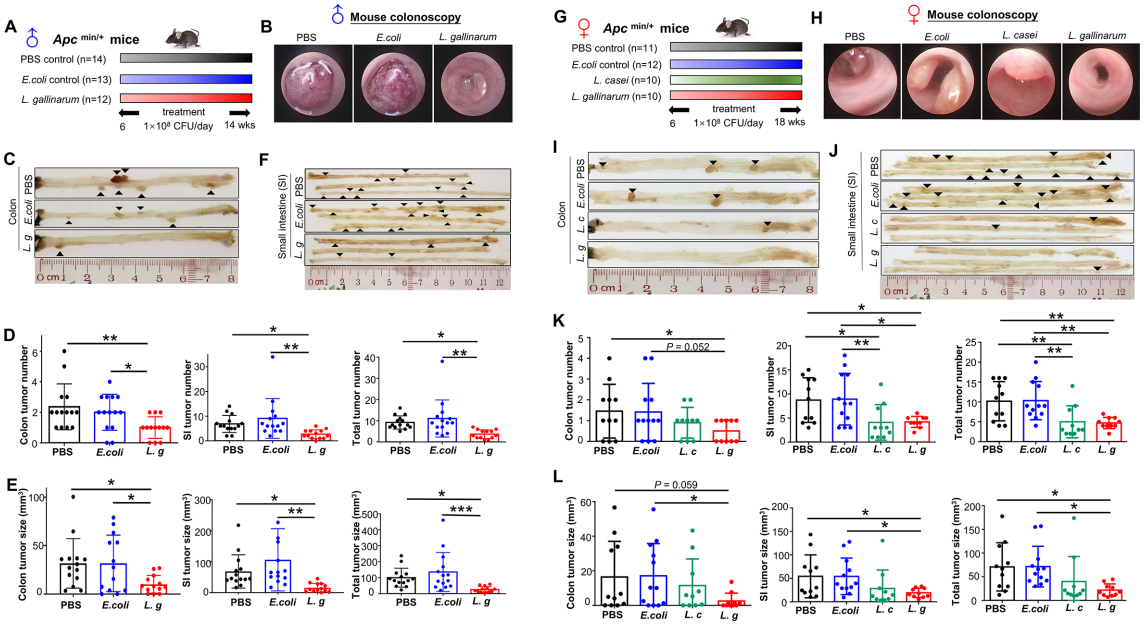

Figure 1 *L. gallinarum* protects against intestinal tumourigenesis in *Apc*$^{Min/+}$ mice. (A) Schematic diagram showing the experimental design, timeline of male *Apc*$^{Min/+}$ mouse model. (B) Representative images of colon tumour from male *Apc*$^{Min/+}$ mouse model. Colonoscopy confirmed that colon tumour size in *L. gallinarum* group was visually smaller than tumours in *Escherichia coli* MG1655 or PBS control groups. In both *E. coli* MG1655 and PBS control groups, colonoscope could not pass through the tumours. (C) Representative macroscopic images of colons from male *Apc*$^{Min/+}$ mouse model. (D) Colon, small intestinal and total tumour number (colon+small intestinal) in male *Apc*$^{Min/+}$ mice under different treatments. (E) Colon, small intestinal and total tumour size (colon+small intestinal) in male *Apc*$^{Min/+}$ mice under different treatments. (F) Representative macroscopic images of small intestines from male *Apc*$^{Min/+}$ mouse model. (G) Schematic diagram showing the experimental design, timeline of female *Apc*$^{Min/+}$ mouse model. (H) Representative colonoscopic images of colon tumour from female *Apc*$^{Min/+}$ mouse model. (I) Representative macroscopic images of colons from female *Apc*$^{Min/+}$ mouse model. (J) Representative macroscopic images of small intestines from female *Apc*$^{Min/+}$ mouse model. (K) Colon, small intestinal and total tumour number (colon+small intestinal) in female *Apc*$^{Min/+}$ mice under different treatments. (L) Colon, small intestinal and total tumour size (colon+small intestinal) in female *Apc*$^{Min/+}$ mice under different treatments. Each black triangle indicates one tumour location. P values are calculated by one-way analysis of variance. *P<0.05, **p<0.01, ***p<0.001. *L. c*, *Lactobacillus casei; L. g*, *Lactobacillus gallinarum*; PBS, phosphate-buffered saline; SI, small intestine.

7-AAD staining distinguished early apoptotic cells (Annexin V$^+$, 7-AAD$^-$) and late apoptotic cells (Annexin V$^+$, 7-AAD$^+$). For cell cycle analysis, cells treated with 10% LGCS, ECCS or BHI for 1 day were fixed and stained with 50 µg/mL propidium iodide (BD Pharmingen). Cell cycle of all stained cells were analysed using FASAria cell sorter (BD Biosciences, San Jose, California, USA).

Liquid chromatography mass spectrometry (LC-MS/MS)-tandem mass spectrometry analysis for bacteria culture supernatant

To investigate anti-CRC metabolites in LGCS, 100 µL of each sample (LGCS, ECCS, BHI) was added to 400 µL extraction solution containing internal standard (L-2-chlorophenylalanine, 2 µg/mL). Following centrifugation, 75 µL of supernatant was transferred to a fresh glass vial for liquid chromatography mass spectrometry (LC-MS/MS) analysis. Ultra-high performance liquid chromatography (UHPLC) separation was carried out using a 1290 Infinity series UHPLC System (Agilent Technologies, Palo Alto, California, USA), equipped with a UPLC BEH Amide column. The analysis was carried with elution gradient as follows: 0–0.5 min, >95% B; 0.5–7.0 min, 95%–65% B; 7.0–8.0 min, 65%–40% B; 8.0–9.0 min, <40% B; 9.0–9.1 min, 40%–95% B; 9.1–12.0 min, 95% B. The TripleTOF 6600 mass spectrometry (AB Sciex, Foster city, California, USA) was used to acquire tandem mass spectrometry (MS/MS) spectra on an information-dependent basis during LC-MS/MS experiment. The processing of LC-MS/MS raw data was achieved using R package XCMS (V.3.2). Peak annotation was processed by CAMERA package implemented in the R language. In-house MS2 database, Human Metabolome Database (HMDB, www.hmdb.ca), and METLIN metabolite database (metlin.scripps.edu) were used for a more reliable metabolite identification. Significantly enriched metabolites were identified by a two-tailed Mann-Whitney U test. Compared with BHI or ECCS, specific metabolite enriched in LGCS with adjusted p value <0.05 was considered statistically significant.

Statistical analysis

Values are expressed as mean±SD for both *in vivo* and *in vitro* experiments. Comparisons between two groups were performed using a two-sided Student's t-test. ANOVA was used to compare differences among multiple groups, and post hoc analysis was performed by Tukey's multiple comparisons test. P value <0.05 indicates statistical significance.

Additional methods are provided in the online supplemental material 1.

RESULTS

L. gallinarum protects against intestinal tumourigenesis in *Apc*$^{Min/+}$ mice

To investigate the effect of *L. gallinarum* on colorectal tumourigenesis, we first used male *Apc*$^{Min/+}$ mice. We gavaged the mice with *L. gallinarum* (1.0×10^8 CFUs per mouse), a non-tumourigenic

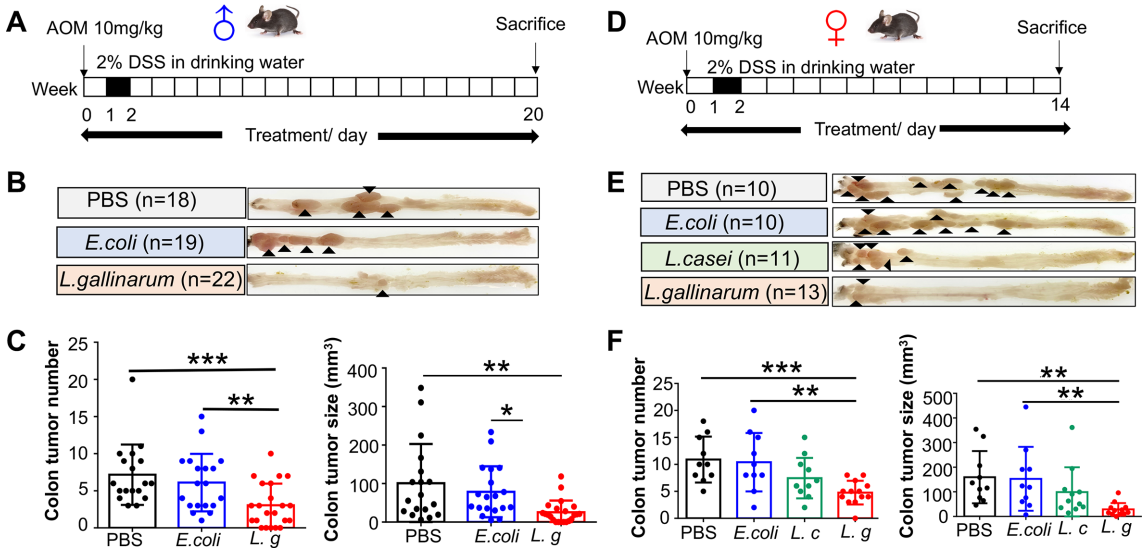

Figure 2 *L. gallinarum* protects against intestinal tumourigenesis in AOM/DSS-induced CRC mice. (A) Schematic diagram showing the experimental design, timeline of male AOM/DSS mouse model. (B) Representative images of colon tumour from male AOM/DSS mouse model. (C) Colon tumour number and tumour size in male AOM/DSS mice under different treatments. (D) Schematic diagram showing the experimental design, timeline of female AOM/DSS mouse model. (E) Representative images of colon tumour from female AOM/DSS mouse model. (F) Colon tumour number and tumour size in female AOM/DSS mice under different treatments. Each black triangle indicates one tumour location. P values are calculated by one-way analysis of variance. *P<0.05, **p<0.01, ***p<0.001. AOM, azoxymethane; DSS, dextran sulfate sodium; *L. c*, *Lactobacillus casei; L. g*, *Lactobacillus gallinarum*; PBS, phosphate-buffered saline; SI, small intestine.

E. coli strain MG1655 (1.0×10^8 CFUs per mouse) as bacteria control, or PBS once daily for 8 weeks (figure 1A). During the period of gavage, there was no difference in body weight among groups (online supplemental figure 1A). The incidence of bloody stool in *L. gallinarum* group was lower than that of the PBS group (p<0.05) after gavage for 8 weeks (online supplemental figure 1B). Colonoscopy identified that colon tumour sizes in *L. gallinarum* group were visually smaller than the *E. coli* MG1655 or PBS groups (figure 1B). After sacrifice (figure 1C), significant reductions in tumour number (*E. coli*, p=0.034; PBS, p=0.005) (figure 1D) and tumour size (figure 1E) (*E. coli*, p<0.05; PBS, p<0.05). *L. gallinarum* also significantly decreased tumour number (*E. coli*, p=0.003; PBS, p<0.05) (figure 1D) and tumour size (*E. coli*, p=0.0012; PBS, p<0.05) (figure 1E) in the small intestine of $Apc^{Min/+}$ mice (figure 1F).

To determine if the protective effect of *L. gallinarum* against CRC is gender-specific, we repeated the experiment in female $Apc^{Min/+}$ mice (figure 1G). *L. casei*, a well-known LAB which has been reported to inhibit CRC progression through releasing small molecules,[20] was used as a positive control. We observed consistent results as in the male $Apc^{Min/+}$ mice, including decreased tumour development as captured by colonoscopy (figure 1H) and tumour incidence in colon (figure 1I) and small intestine (figure 1J) in *L. gallinarum*-treated female $Apc^{Min/+}$ mice. Significant reductions of both total tumour number (*L. gallinarum* vs *E. coli*, p<0.01; *L. gallinarum* vs PBS, p<0.01) and total tumour size (*L. gallinarum* vs *E. coli*, p<0.05; *L. gallinarum* vs PBS, p<0.05) were also observed in *L. gallinarum*-treated female $Apc^{Min/+}$ mice as compared with controls (figure 1K and L, online supplemental figure 2). Accordingly, *L. casei* slightly inhibited tumour formation in female $Apc^{Min/+}$ mice (figure 1K), but its effect was not as strong as that of *L. gallinarum*. These results suggested that *L. gallinarum* abrogates intestinal tumourigenesis in both male and female $Apc^{Min/+}$ mice.

L. gallinarum protects against intestinal tumourigenesis in AOM/DSS-induced CRC mice

To validate the tumor-suppressive effect of *L. gallinarum* on colorectal tumourigenesis, we established a colitis-associated CRC model, in which C57BL/6 mice aged 6 weeks were intraperitoneally injected with 10 mg/kg AOM, followed by 2% DSS administration for 1 week (figure 2A). *L. gallinarum* significantly reduced colorectal tumour number (*E. coli*, p<0.05; PBS, p=0.007) and tumour size (*E. coli*, p=0.019; PBS, p=0.0013) (figure 2B and C) in AOM/DSS-induced male CRC mice. Consistently, same results were observed in AOM/DSS-induced female CRC mice (figure 2D–F). During the period of gavage, there was no difference in body weight among different groups of mice (online supplemental figure 3 and online supplemental figure 4), indicating that *L. gallinarum* suppresses intestinal tumourigenesis in AOM/DSS-induced CRC in both male and female mice.

L. gallinarum modulates the gut microbiota of $Apc^{Min/+}$ mice

To investigate the effects of *L. gallinarum* on gut microbiota, we performed 16S rDNA gene sequencing on $Apc^{Min/+}$ mouse stool samples after gavage of *L. gallinarum* for 8 weeks. The microbial abundance in *L. gallinarum* group significantly increased compared with PBS (p<0.05), while there was no difference between *L. gallinarum* and *E. coli* groups (figure 3A). Similarly, although the β-diversity of stool samples from *L. gallinarum*-gavaged mice had a distinct trend compared with other two groups, there was no statistical significance (figure 3B). However, *L. gallinarum* could enhance abundances of some well-characterised commensal probiotics including *Lactobacillus helveticus*, *Lactobacillus reuteri* and OTUs from the Bacteroidetes phylum (figure 3C). Moreover, some genera, such as *Alistipes*, *Allobacullum*, *Dorea*, *Odoribacter*, *Parabacteroides* and *Ruminococcus* with species of pathogenic potentials, exhibited significantly decreased abundances in mice treated with *L. gallinarum* compared with control groups (figure 3C). Taken

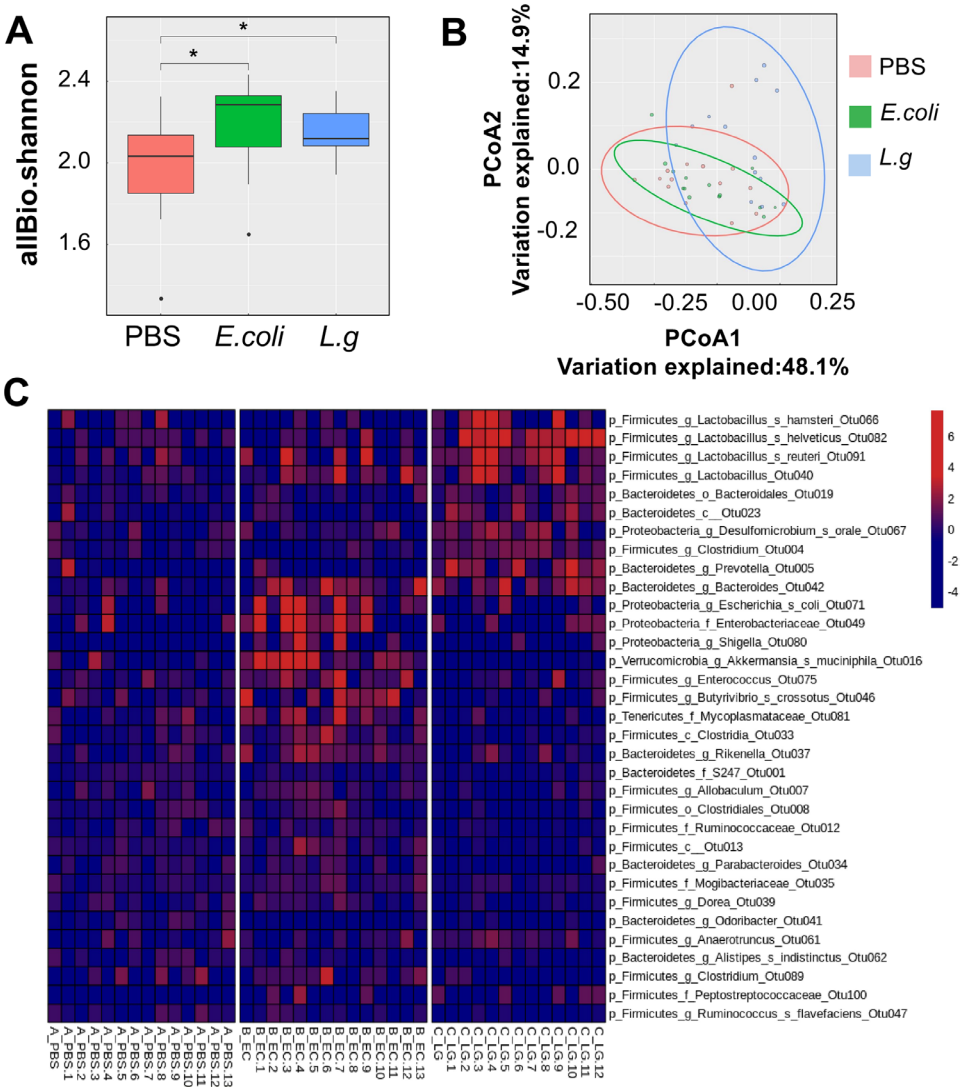

Figure 3 *L. gallinarum* modulates the gut microbiota of *Apc*$^{Min/+}$ mice. 16S rDNA gene analysis of intestinal microbiome. (A) Alpha-diversity analysis of luminal microbiota OTU at various taxonomic ranks. (B) Principal coordinate analysis (PCoA) of β-diversity based on Bray-Curtis dissimilarity matrix of OTU-level compositional profiles. Ellipses represent 95% CIs. Solid diamond-shaped points in black denote species scores, which were calculated using the *vegan* R-CRAN package. (C) Heatmap of differentially abundant bacterial OTUs using one-way analysis of variance, at p<0.05. *L. g*, *L. gallinarum*; OTU, operational taxonomic unit.

together, although *L. gallinarum* could not change the overall gut microbiota composition, it could enrich abundances of probiotics and potentially deplete gut pathogens.

L. gallinarum supernatant inhibits the viability of colon cancer cells

To validate the tumor-suppressive effect of *L. gallinarum in vivo*, we performed *in vitro* functional analyses using two CRC cell lines (HCT116 and LoVo) and a normal colonic epithelial cell line (NCM460) as control. Treatment with the culture supernatant of *L. gallinarum* significantly reduced the viability of CRC cell lines in a concentration-dependent manner, but not in normal colonic epithelial cell line as determined by cell viability assay (figure 4A–C). Similar results were observed in colony formation assay in which HCT116 (ECCS, p=0.0002; BHI, p=0.0003) and LoVo (ECCS, p=0.0001; BHI, $p=7.6\times10^{-5}$) showed significant decrease in colony compared with ECCS or BHI groups (figure 4D). These data indicated that the secreted molecules from *L. gallinarum* could suppress viability and colony-forming ability of CRC cells.

L. gallinarum supernatant promotes apoptosis in CRC cells

To determine the mechanism by which LGCS suppresses CRC cell viability, the effects of LGCS on apoptosis and cell cycle distribution were assessed quantitatively by flow cytometry with Annexin V-PE and 7-AAD staining. We found that LGCS significantly promoted apoptosis in CRC cell lines, HCT116 (ECCS, $p=3.3\times10^{-6}$; BHI, $p=5.1\times10^{-6}$) (figure 5A) and LoVo (ECCS, $p=1.4\times10^{-6}$; BHI, $p=3.6\times10^{-6}$) (figure 5B), while it had no effect on normal epithelial colonic cells, NCM460 (figure 5C). Moreover, we confirmed this apoptosis-inducing property of LGCS on CRC organoids derived from 2 patients, 74 (ECCS, $p=1.2\times10^{-5}$; BHI, p=0.0001) and 816 (ECCS, p=0.0013; BHI, p=0.0016) (figure 5D and E). By contrast, LGCS had no effect on cell cycle distribution in CRC cells (figure 5F–H).

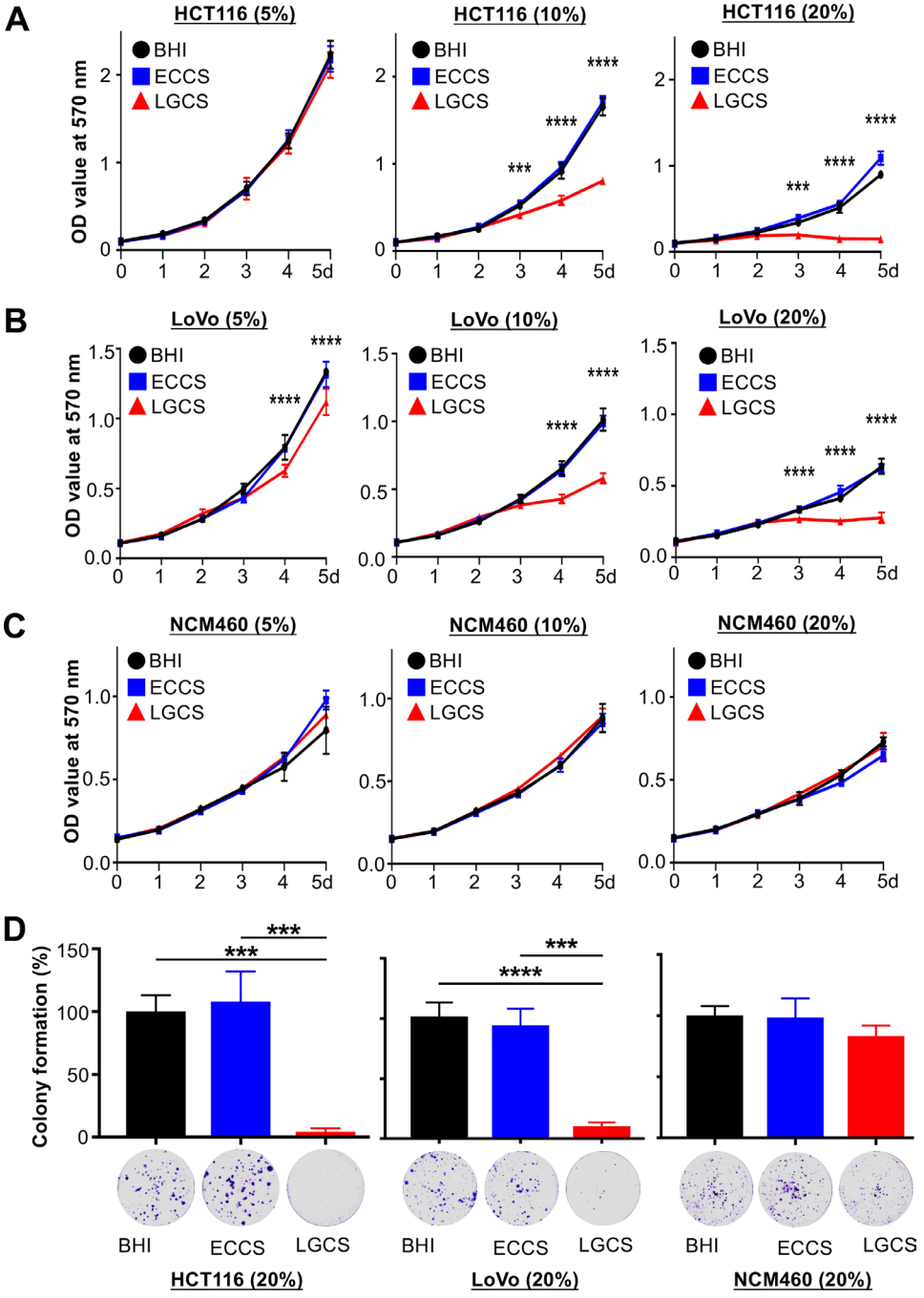

Figure 4 *L. gallinarum* supernatant inhibits the viability of colon cancer cells. The proliferation of cells was measured by 3-(4,5-dimethylthiazoly-2-yl)-2,5-diphenyltetrazolium bromide assay. Different concentrations of culture supernatant were used for culturing CRC cell lines, HCT116 (5%, 10%, 20%) and LoVo (5%, 10%, 20%) and normal colonic epithelial cell line, NCM460 (5%, 10%, 20%). (A) The culture supernatant of *L. gallinarum*, especially in 10% and 20%, significantly suppressed the cell growth of HCT116 from day 4 to day 5. (B) The cell growth of LoVo was also significantly suppressed by the culture supernatant of *L. gallinarum* with different concentrations; both 5% and 10% from day 4 to day 5, and 20% from day 3 to day 5. (C) No change in cell growth could be observed in normal colonic epithelial cell line. (D) 20% LGCS suppressed colony formation of CRC cells. P values are calculated by two-way analysis of variance. ***P<0.001, ****p<0.0001. BHI, brain heart infusion; CRC, colorectal cancer; ECCS, *Escherichia coli* culture supernatant; LGCS, *Lactobacillus gallinarum* culture supernatant.

Antitumour molecules produced from *L. gallinarum* are non-protein with a molecular weight <3 kDa

To investigate the features of anti-CRC molecules produced from *L. gallinarum*, bacterial culture supernatant was separated into low molecular weight (LMW) (<3 kDa) and high molecular weight (HMW) (>3 kDa) fractions using 3 kDa filter units. We found that decrease in viability of CRC cells was observed only in those treated with LGCS LMW fraction, while LGCS HMW fraction had no suppressive effect on CRC cells (figure 6A). Meanwhile, both heat-inactivated LGCS (figure 6B) and proteinase K-treated LGCS (figure 6C) retained the ability to reduce cell viability of CRC cells. Collectively, these results indicated that the anti-CRC properties of *L. gallinarum* could be induced by non-protein molecules with a molecular weight <3 kDa.

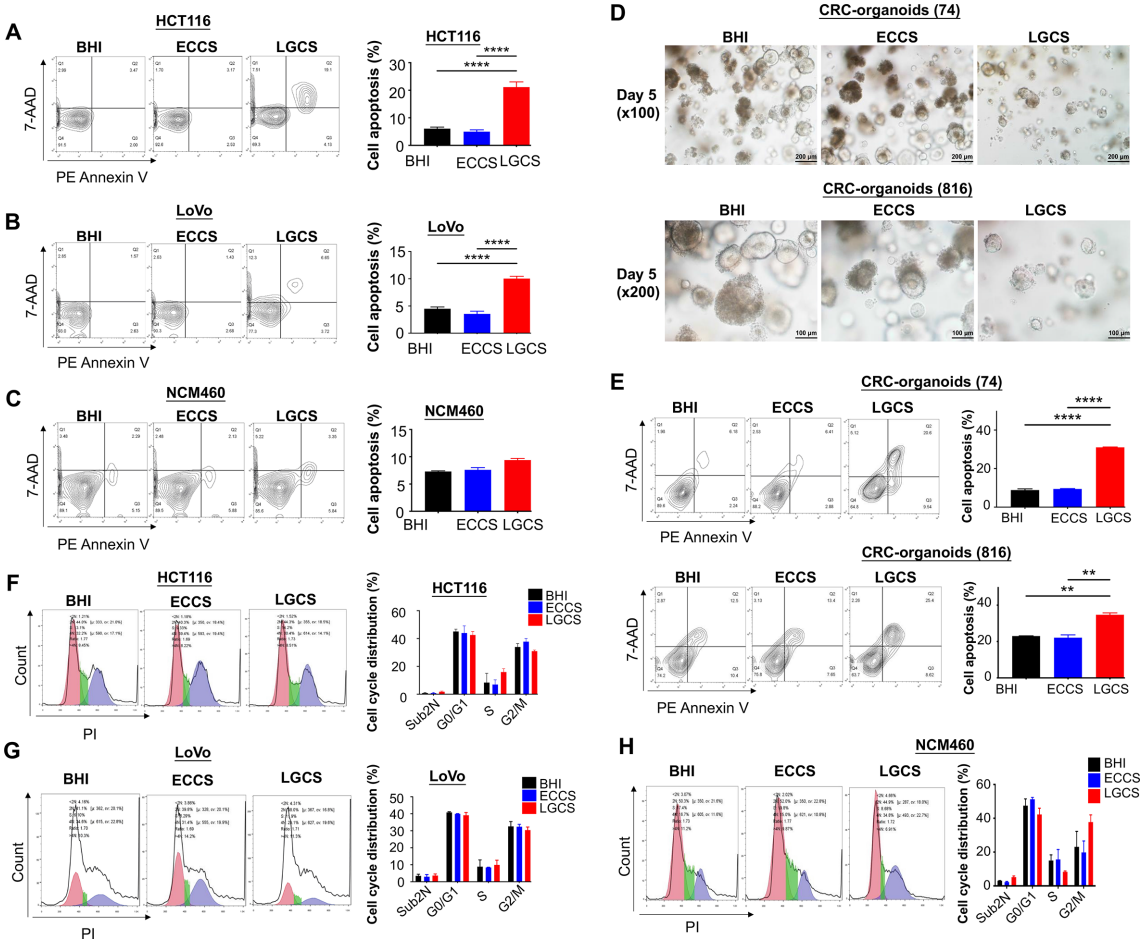

Figure 5 *L. gallinarum* supernatant promotes apoptosis instead of cell cycle arrest in CRC cells. (A) LGCS significantly promoted apoptosis including both early and late phases in two CRC cell lines HCT116, and (B) LoVo, but not in the normal colonic epithelial cell line (C) NCM460. (D) The size and number of CRC patient-derived organoids was visually reduced in medium containing 10% LGCS. (E) LGCS significantly promoted apoptosis including both early and late phases in CRC patient-derived organoids. (F) LGCS had no effect on cell cycle distribution in HCT116, (G) LoVo and (H) NCM460. P values are calculated by one-way analysis of variance. **P<0.01, ****p<0.0001. BHI, brain heart infusion; CRC, colorectal cancer; ECCS, *Escherichia coli* culture supernatant; LGCS, *Lactobacillus gallinarum* culture supernatant; PI, propidium iodide.

We next performed non-targeted LC-MS/MS to identify anti-CRC metabolite(s) in the LGCS-LMW fraction (online supplemental table 2). Score plots of principal component analysis (PCA) showed clear separations among LMW fractions of LGCS, ECCS and BHI groups (figure 6D). Differential abundance analysis showed the critical products generated from *L. gallinarum* that may contribute to the anti-CRC effects (figure 6E). To verify if *L. gallinarum*-produced LMW molecules are responsible for the anti-CRC effect *in vivo*, we then examined the intestine metabolomics by using faecal samples from $Apc^{Min/+}$ mice under different treatments (online supplemental table 3). Daily administration of *L. gallinarum* caused a significant overall compositional alteration of the gut metabolites as revealed by principal coordinate analysis (figure 6F). We found that metabolites including L-tryptophan, palmitic acid, 4-pyridoxic acid and gamma-L-glutamyl-L-glutamic acid were significantly upregulated in mice after *L. gallinarum* gavage as compared with control groups (figure 6G), which were also highly upregulated in LGCS (figure 6E). Among them, L-tryptophan was the most upregulated metabolite secreted by *L. gallinarum*. L-tryptophan is commonly converted into its downstream metabolites by gut microbiota.[21] We anticipated that *L. gallinarum*-produced L-tryptophan and its downstream metabolites could be responsible for the anti-CRC effect exhibited by *L. gallinarum*.

L. gallinarum produces and catabolises L-tryptophan to release indole-3-lactic acid to protect against CRC

To further confirm L-tryptophan production by *L. gallinarum* and its conversion into downstream metabolites, we performed high-throughput targeted L-tryptophan metabolic profiling using culture supernatant at the late-stage stationary phase of *L. gallinarum* to ensure sufficient release and metabolic conversion of the metabolites (online supplemental table 4), as well as faecal samples from $Apc^{Min/+}$ mice (online supplemental table 5). The PCA plot regarding L-tryptophan and its downstream metabolites showed obvious separations among LGCS, ECCS and BHI (figure 7A). Stool samples from *L. gallinarum*-treated $Apc^{Min/+}$ mice also displayed clear separations from *E. coli*-treated or PBS mice (figure 7B). Differential abundance analysis showed that, in contrast to the log-phase culture supernatant, L-tryptophan was decreased in the stationary-phase LGCS (figure 7C), suggesting that *L. gallinarum* could catabolise L-tryptophan. In particular, we found ILA, which is one of the downstream catabolites from L-tryptophan, was highly enriched in both LGCS (figure 7C) and stool samples from *L. gallinarum*-tretaed $Apc^{Min/+}$ mice (figure 7D).

We then performed functional investigation of ILA in CRC cell growth *in vitro* and in CRC tumourigenesis *in vivo*. As shown in

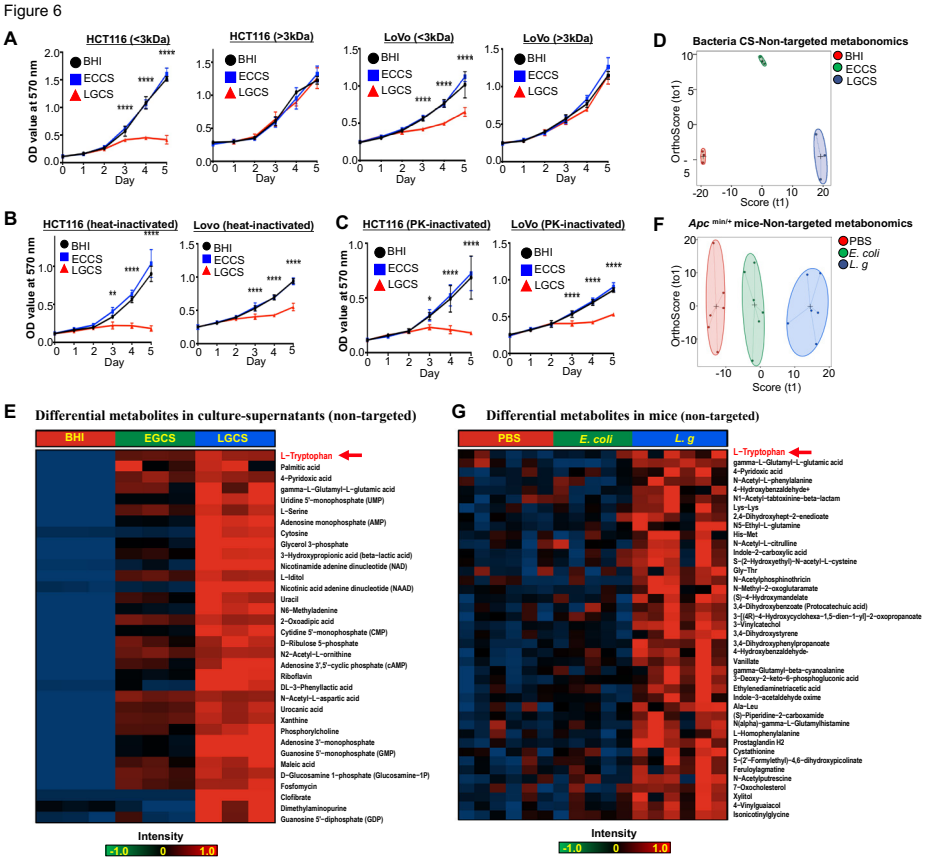

Figure 6 Antitumour molecules produced from *L. gallinarum* are non-protein with a molecular weight <3 kDa. (A) LMW-LGCS but not HMW-LGCS significantly suppressed cell growth of HCT116 and LoVo. (B) Decrease in proliferation of CRC cells was observed in heat-inactivated LGCS. (C) Decrease in proliferation of CRC cells was observed in PK-inactivated LGCS. (D) Score plots of PCA revealed clear separations of metabolites in culture supernatant of *L. gallinarum*, *E. coli* MG1655 and BHI groups. (E) Heatmap analysis revealed the abundance of different metabolites in LGCS, ECCS and BHI groups . (F) Score plots of PCA revealed clear separations among *L. gallinarum*, *E. coli* MG1655 and PBS-treated $Apc^{Min/+}$ mice. (G) Heatmap analysis revealed the abundance of different metabolites in the gut of $Apc^{Min/+}$ mice under different treatments. P values are calculated by two-way analysis of variance or Student's t-test as appropriate. *P<0.05, **p<0.01, ****p<0.0001. BHI, brain heart infusion; CRC, colorectal cancer; ECCS, *Escherichia coli* culture supernatant; HMW, high molecular weight; LGCS, *Lactobacillus gallinarum* culture supernatant; LMW, low molecular weight; PBS, phosphate-buffered saline; PCA, principal component analysis; PK, proteinase K.

figure 7E, cell viability of CRC cells (HCT116 and LoVo) but not normal colonic epithelial cell NCM460 was substantially reduced when exposing to ILA at a concentration comparable to that of LGCS. Consistent with the effect of LGCS, ILA-treated CRC cells showed an increase in apoptosis (figure 7F). For *in vivo* experiments, gavage of ILA (20 mg/kg) into $Apc^{Min/+}$ mice (figure 7G) significantly reduced tumour number (figure 7H) and tumour size (figure 7I). The amount of cells with positive TUNEL staining was also increased in ILA-treated tumour tissues, but not in adjacent normal tissues (figure 7J). Moreover, we have performed additional experiments to investigate if antagonising ILA could abrogate *L. gallinarum* medicated anticancer effect. As shown in online supplemental figure 6A, blocking ILA receptor, AhR, using AhR antagonist (CH-223191)[22 23] abolished the effect of *L. gallinarum* in suppressing CRC *in vitro* (online supplemental figure 6B) and in $Apc^{Min/+}$ mice (online supplemental figure 6C-6H). Collectively, these data suggested that *L. gallinarum* could produce L-tryptophan, and at the same time, convert it to its downstream ILA and other metabolites. Thus, ILA could contribute, at least in part, to the tumor-suppressive effect of *L. gallinarum*.

DISCUSSION

In this study, we demonstrated for the first time that oral administration of *L. gallinarum* reduced intestinal tumour number and size in $Apc^{Min/+}$ mice and confirmed in AOM/DSS-induced CRC mouse model, indicating that *L. gallinarum* suppresses CRC tumourigenesis in both male and female mice. From *in vitro* experiments, we found that small non-protein metabolites produced by *L. gallinarum* suppressed the growth of CRC cells and CRC patient-derived organoids by promoting apoptosis.

Certain probiotics can suppress the progression of CRC in preclinical experiments.[24–29] For example, both living and heat-killed *L. rhamnosus* GG (LGG) have anti-CRC effect by promoting apoptosis in human CRC cells.[30] In an animal model, LGG could suppress CRC development by increasing expressions of various pro-apoptotic proteins such as Bax, casp3 and p53.[31] Several studies have suggested that regular consumption of probiotics may improve the imbalanced intestinal microbiota, thus reducing the chance of chronic inflammation and production of carcinogenic compounds during intestinal dysbiosis.[32–34]

In the present study, we found that *L. gallinarum* significantly enriched the abundance of well-characterised commensal probiotics, such as *L. helveticus* and *L. reuteri*. While some

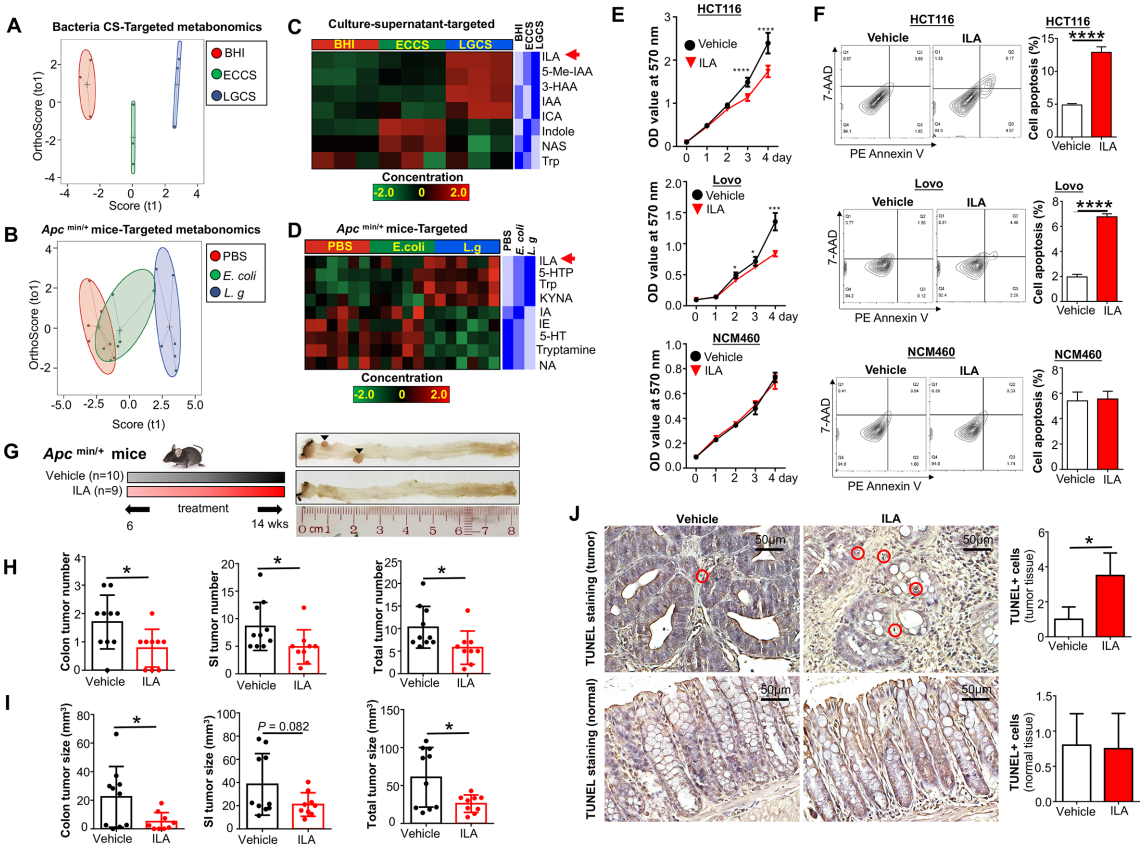

Figure 7 *L. gallinarum* produces and catabolises L-tryptophan to release ILA to protect against CRC. Targeted metabonomics on L-tryphtophan were performed on different culture supernatants and faecal samples from *Apc*$^{Min/+}$ mice under different treatments. (A) Score plots of PCA revealed clear separations among culture supernatant of *L. gallinarum*, *E. coli* MG1655 and BHI groups. (B) Score plots of PCA revealed clear separations among faecal samples from *L. gallinarum*-treated, *E. coli* MG1655-treated and PBS *Apc*$^{Min/+}$ mice. (C) Heatmap analysis revealed the abundance of different metabolites in LGCS, ECCS and BHI groups. (D) Heatmap analysis revealed the abundance of different metabolites in the gut of *Apc*$^{Min/+}$ mice under different treatments. (E) The cell growth of CRC cells was significantly suppressed by ILA. (F) The cell apoptosis of CRC cells was significantly increased by ILA. (G) Schematic diagram showing the experimental design, timeline and representative macroscopic images of colons from of ILA-treated *Apc*$^{Min/+}$ mouse model. (H) Colon, small intestinal and total tumour number (colon+small intestinal) in *Apc*$^{Min/+}$ mice with or without ILA treatment. (I) Colon, small intestinal with or without ILA treatment. (J) TUNEL-positive staining cells in colon tissues of *Apc*$^{Min/+}$ mice with or without ILA treatment. Each black triangle indicates one tumour location. P values are calculated by two-way analysis of variance or Student's t-test as appropriate. *P<0.05, **p<0.01, ****p<0.0001. BHI, brain heart infusion; CRC, colorectal cancer; ECCS, *Escherichia coli* culture supernatant; ILA, indole-3-lactic acid; LGCS, *Lactobacillus gallinarum* culture supernatant; PBS, phosphate-buffered saline; PCA, principal component analysis.

potential pathogenic species, such as *Alistipes*, *Allobacullum*, *Dorea*, *Odoribacter*, *Parabacteroides* and *Ruminococcus*,[35–37] were significantly depleted in mice treated with *L. gallinarum*, *L. reuteri* is known to suppress inflammation-associated colon carcinogenesis by producing histamine.[38] Thus, *L. gallinarum* suppresses CRC at least in part through enriching abundances of probiotics and depleting potential CRC pathogens. Gut microbiota plays a critical role in CRC tumourigenesis. Our previous study showed that transplantation of faeces from patients with CRC can promote tumourigenesis in germ-free mice and AOM-treated mice.[39] Another study demonstrated that transplantation of faecal samples from AOM/DSS mice to germ-free mice led to increased tumour development compared with those harbouring faecal samples from naïve healthy mice.[40] These studies suggest that gut dysbiosis contributes to tumour susceptibility and alteration of the intestinal microbiota is an important determinant of colon tumourigenesis. Meanwhile, some studies found that probiotics can alter the composition of microbiota to alleviate cancer progression. For example, *Lactobacillus salivarius* Ren could suppress CRC tumourigenesis via modulating intestinal microbiota.[41 42] These findings collectively inferred that probiotics like *L. gallinarum* suppress CRC development through modulating gut microbial composition.

We also demonstrated that metabolites produced by *L. gallinarum* could suppress CRC cell viability through inducing apoptosis. Using metabolomic analysis, we found that *L. gallinarum* could produce L-tryptophan and convert L-tryptophan to its catabolites. We further identified that ILA, one of the L-tryptophan catabolites, was significantly increased in both LGCS and faecal samples of *L. gallinarum*-treated *Apc*$^{Min/+}$ mice. ILA inhibited CRC cell viability *in vitro* and suppressed intestinal tumour development *in vivo*. A recent report suggested that L-tryptophan catabolites generated by the gut microbiota are important contributors in maintaining intestinal homeostasis.[21] ILA was identified as a metabolite of breastmilk tryptophan, secreted by the probiotic *Bifidobacterium longum* to prevent inflammation.[23] Production of ILA from gut microbes was reported to alleviate colitis in mice through inhibiting epithelial autophagy.[43] ILA was also found to have regulatory effect on intestinal innate immunity, which plays a specific role in host-microbe crosstalk. CRC is influenced by the balance between microbial production of health-promoting metabolites (eg, short-chain fatty acids) and

potentially carcinogenic metabolites (eg, secondary bile acids).[44] Previous studies demonstrated the anticarcinogenic attributes of probiotic metabolites, especially for those produced by LAB.[45 46] For example, metabolites produced by *Lactobacillus plantarum* exhibited selective cytotoxicity via provoking anti-proliferative activity and inducing apoptosis against malignant cancer cells.[47] Ferrichrome derived from *L. casei* has a strong tumour-suppressive effect on CRC cells by inhibiting the JNK signalling pathway.[20] Interestingly, we also observed stronger tumor-suppressive effect of LGCS as compared with LCCS (online supplemental figure 5). Thus, the anti-CRC feature of *L. gallinarum* could be also at least in part attributed to its released protective metabolites. However, whether ILA secreted from *L. gallinarum* is the main metabolite for CRC suppression requires further investigation.

In conclusion, to our understanding, this is the first study to demonstrate the anti-CRC effect of *L. gallinarum*. *L. gallinarum* protects against intestinal tumourigenesis. Such action is associated with modulation of the gut microbial composition and secretion of protective metabolites including ILA to promote apoptosis of cancer cells. These findings may facilitate the development of therapeutic strategy using probiotics for prevention of CRC.

Author affiliations
[1]Institute of Digestive Disease and Department of Medicine and Therapeutics, State Key Laboratory of Digestive Disease, Li Ka Shing Institute of Health Sciences, CUHK-Shenzhen Research Institute, The Chinese University of Hong Kong, Hong Kong, China
[2]Department of Gastroenterology, Osaka City University Graduate School of Medicine, Osaka, Japan
[3]Department of Anaesthesia and Intensive Care and Peter Hung Pain Research Institute, The Chinese University of Hong Kong, Hong Kong, China
[4]Institute of Precision Medicine, the First Affiliated Hospital, Sun Yat-sen University, Guangzhou, China
[5]Department of Immunology and Infectious Diseases/Genetics and Complex Disease, Harvard T. H. Chan School of Public Health, Boston, Massachusetts, USA

Contributors NS and QL were involved in study design, conducted the experiments and drafted the paper; ESHC, HCHL, WF, CL and ACYS performed the experiments; WXL, GN and OOC performed bioinformatics analyses; WKKW commented and revised the manuscript; FKLC supervised NS and commented on the study; JY designed, supervised the study and revised the manuscript.

Funding This study was supported by National Key R&D Programme of China (No. 2020YFA0509200/2020YFA0509203), RGC Theme-based Res Scheme Hong Kong (T21-705/20-N), Lim Peng Suan Charitable Trust Research Grant Hong Kong, RGC-CRF Hong Kong (C4039-19GF, C7065-18GF), RGC-GRF Hong Kong (14163817), Research Impact Fund Hong Kong (R4017-18F), Vice-Chancellor's Discretionary Fund Chinese University of Hong Kong.

Competing interests None declared.

Patient consent for publication Not applicable.

Ethics approval This study does not involve human participants. All animal studies were performed in accordance with guidelines approved by the Animal Experimentation Ethics Committee of The Chinese University of Hong Kong.

Provenance and peer review Not commissioned; externally peer reviewed.

Data availability statement All data relevant to the study are included in the article or uploaded as supplementary information.

ORCID iDs
Harry Cheuk Hay Lau http://orcid.org/0000-0003-3581-2909
William Ka Kei Wu http://orcid.org/0000-0002-5662-5240
Francis Ka Leung Chan http://orcid.org/0000-0001-7388-2436
Jun Yu http://orcid.org/0000-0001-5008-2153

REFERENCES

1 Siegel RL, Miller KD, Jemal A. Cancer statistics, 2019. *CA Cancer J Clin* 2019;69:7–34.
2 Rawla P, Sunkara T, Barsouk A. Epidemiology of colorectal cancer: incidence, mortality, survival, and risk factors. *Prz Gastroenterol* 2019;14:89–103.
3 Li Q, Hu W, Liu W-X, *et al*. Streptococcus thermophilus inhibits colorectal tumorigenesis through secreting β-galactosidase. *Gastroenterology* 2021;160:1179–93.
4 Mao J, Qi S, Cui Y, *et al*. Lactobacillus rhamnosus GG attenuates lipopolysaccharide-induced inflammation and barrier dysfunction by regulating MAPK/NF-κB signaling and modulating metabolome in the piglet intestine. *J Nutr* 2020;150:1313–23.
5 Lin R, Sun Y, Mu P, *et al*. Lactobacillus rhamnosus GG supplementation modulates the gut microbiota to promote butyrate production, protecting against deoxynivalenol exposure in nude mice. *Biochem Pharmacol* 2020;175:113868.
6 Soltan Dallal MM, Mojarrad M, Baghbani F, *et al*. Effects of probiotic Lactobacillus acidophilus and Lactobacillus casei on colorectal tumor cells activity (Caco-2). *Arch Iran Med* 2015;18:167–72.
7 Zhuo Q, Yu B, Zhou J, *et al*. Lysates of Lactobacillus acidophilus combined with CTLA-4-blocking antibodies enhance antitumor immunity in a mouse colon cancer model. *Sci Rep* 2019;9:20128.
8 Salva S, Marranzino G, Villena J, *et al*. Probiotic Lactobacillus strains protect against myelosuppression and immunosuppression in cyclophosphamide-treated mice. *Int Immunopharmacol* 2014;22:209–21.
9 Shin R, Itoh Y, Kataoka M, *et al*. Anti-Tumor activity of heat-killed Lactobacillus plantarum BF-LP284 on Meth-A tumor cells in BALB/c mice. *Int J Food Sci Nutr* 2016;67:641–9.
10 Dai Z, Coker OO, Nakatsu G, *et al*. Multi-Cohort analysis of colorectal cancer metagenome identified altered bacteria across populations and universal bacterial markers. *Microbiome* 2018;6:70.
11 Moser AR, Pitot HC, Dove WF. A dominant mutation that predisposes to multiple intestinal neoplasia in the mouse. *Science* 1990;247:322–4.
12 Sápi J, Kovács L, Drexler DA, *et al*. Tumor volume estimation and quasi-continuous administration for most effective bevacizumab therapy. *PLoS One* 2015;10:e0142190.
13 Schloss PD, Westcott SL, Ryabin T, *et al*. Introducing mothur: open-source, platform-independent, community-supported software for describing and comparing microbial communities. *Appl Environ Microbiol* 2009;75:7537–41.
14 Needleman SB, Wunsch CD. A general method applicable to the search for similarities in the amino acid sequence of two proteins. *J Mol Biol* 1970;48:443–53.
15 Quast C, Pruesse E, Yilmaz P, *et al*. The Silva ribosomal RNA gene database project: improved data processing and web-based tools. *Nucleic Acids Res* 2013;41:D590–6.
16 DeSantis TZ, Hugenholtz P, Keller K, *et al*. NAST: a multiple sequence alignment server for comparative analysis of 16S rRNA genes. *Nucleic Acids Res* 2006;34:W394–9.
17 Edgar RC, Haas BJ, Clemente JC, *et al*. UCHIME improves sensitivity and speed of chimera detection. *Bioinformatics* 2011;27:2194–200.
18 Dembélé D, Kastner P. Fold change RANK ordering statistics: a new method for detecting differentially expressed genes. *BMC Bioinformatics* 2014;15:14.
19 Jin Y, Tang S, Li W, *et al*. Hemolytic E. coli promotes colonic tumorigenesis in females. *Cancer Res* 2016;76:2891–900.
20 Konishi H, Fujiya M, Tanaka H, *et al*. Probiotic-derived ferrichrome inhibits colon cancer progression via JNK-mediated apoptosis. *Nat Commun* 2016;7:12365.
21 Roager HM, Licht TR. Microbial tryptophan catabolites in health and disease. *Nat Commun* 2018;9:3294.
22 Wong CB, Tanaka A, Kuhara T, *et al*. Potential effects of Indole-3-Lactic acid, a metabolite of human bifidobacteria, on NGF-induced neurite outgrowth in PC12 cells. *Microorganisms* 2020;8. doi:10.3390/microorganisms8030398. [Epub ahead of print: 12 03 2020].
23 Meng D, Sommella E, Salviati E, *et al*. Indole-3-lactic acid, a metabolite of tryptophan, secreted by Bifidobacterium longum subspecies infantis is anti-inflammatory in the immature intestine. *Pediatr Res* 2020;88:209–17.
24 Jan G, Belzacq A-S, Haouzi D, *et al*. Propionibacteria induce apoptosis of colorectal carcinoma cells via short-chain fatty acids acting on mitochondria. *Cell Death Differ* 2002;9:179–88.
25 Tiptiri-Kourpeti A, Spyridopoulou K, Santarmaki V, *et al*. Lactobacillus casei exerts anti-proliferative effects accompanied by apoptotic cell death and up-regulation of TRAIL in colon carcinoma cells. *PLoS One* 2016;11:e0147960.
26 Saxami G, Karapetsas A, Chondrou P, *et al*. Potentially probiotic Lactobacillus strains with anti-proliferative activity induce cytokine/chemokine production and neutrophil recruitment in mice. *Benef Microbes* 2017;8:615–23.

27 Elfahri KR, Vasiljevic T, Yeager T, *et al*. Anti-colon cancer and antioxidant activities of bovine skim milk fermented by selected Lactobacillus helveticus strains. *J Dairy Sci* 2016;99:31–40.
28 El-Deeb NM, Yassin AM, Al-Madboly LA, *et al*. A novel purified Lactobacillus acidophilus 20079 exopolysaccharide, LA-EPS-20079, molecularly regulates both apoptotic and NF-κB inflammatory pathways in human colon cancer. *Microb Cell Fact* 2018;17:29.
29 Agah S, Alizadeh AM, Mosavi M, *et al*. More protection of Lactobacillus acidophilus than Bifidobacterium bifidum probiotics on azoxymethane-induced mouse colon cancer. *Probiotics Antimicrob Proteins* 2019;11:857–64.
30 Orlando A, Refolo MG, Messa C, *et al*. Antiproliferative and proapoptotic effects of viable or heat-killed Lactobacillus paracasei IMPC2.1 and Lactobacillus rhamnosus GG in HGC-27 gastric and DLD-1 colon cell lines. *Nutr Cancer* 2012;64:1103–11.
31 Gamallat Y, Meyiah A, Kuugbee ED, *et al*. Lactobacillus rhamnosus induced epithelial cell apoptosis, ameliorates inflammation and prevents colon cancer development in an animal model. *Biomed Pharmacother* 2016;83:536–41.
32 Hatakka K, Holma R, El-Nezami H, *et al*. The influence of Lactobacillus rhamnosus LC705 together with Propionibacterium freudenreichii ssp. shermanii JS on potentially carcinogenic bacterial activity in human colon. *Int J Food Microbiol* 2008;128:406–10.
33 Ohara T, Yoshino K, Kitajima M. Possibility of preventing colorectal carcinogenesis with probiotics. *Hepatogastroenterology* 2010;57:1411–5.
34 Liu Z, Qin H, Yang Z, *et al*. Randomised clinical trial: the effects of perioperative probiotic treatment on barrier function and post-operative infectious complications in colorectal cancer surgery - a double-blind study. *Aliment Pharmacol Ther* 2011;33:50–63.
35 Jeon H-J, Yeom Y, Kim Y-S, *et al*. Effect of vitamin C on azoxymethane (AOM)/dextran sulfate sodium (DSS)-induced colitis-associated early colon cancer in mice. *Nutr Res Pract* 2018;12:101–9.
36 Koh GY, Kane AV, Wu X, *et al*. Parabacteroides distasonis attenuates tumorigenesis, modulates inflammatory markers and promotes intestinal barrier integrity in azoxymethane-treated A/J mice. *Carcinogenesis* 2020;41:909–17.
37 Song H, Wang W, Shen B, *et al*. Pretreatment with probiotic Bifico ameliorates colitis-associated cancer in mice: transcriptome and gut flora profiling. *Cancer Sci* 2018;109:666–77.
38 Gao C, Ganesh BP, Shi Z, *et al*. Gut Microbe-Mediated suppression of inflammation-associated colon carcinogenesis by luminal histamine production. *Am J Pathol* 2017;187:2323–36.
39 Wong SH, Zhao L, Zhang X, *et al*. Gavage of Fecal Samples From Patients With Colorectal Cancer Promotes Intestinal Carcinogenesis in Germ-Free and Conventional Mice. *Gastroenterology* 2017;153:1621–33.
40 Zackular JP, Baxter NT, Iverson KD, *et al*. The gut microbiome modulates colon tumorigenesis. *mBio* 2013;4:e00692–13.
41 Zhang M, Fan X, Fang B, *et al*. Effects of Lactobacillus salivarius ren on cancer prevention and intestinal microbiota in 1, 2-dimethylhydrazine-induced rat model. *J Microbiol* 2015;53:398–405.
42 Zhu J, Zhu C, Ge S, *et al*. Lactobacillus salivarius ren prevent the early colorectal carcinogenesis in 1, 2-dimethylhydrazine-induced rat model. *J Appl Microbiol* 2014;117:208–16.
43 Fan Q, Guan X, Hou Y, *et al*. Paeoniflorin modulates gut microbial production of indole-3-lactate and epithelial autophagy to alleviate colitis in mice. *Phytomedicine* 2020;79:153345.
44 Ou J, Carbonero F, Zoetendal EG, *et al*. Diet, microbiota, and microbial metabolites in colon cancer risk in rural Africans and African Americans. *Am J Clin Nutr* 2013;98:111–20.
45 Lupton JR. Microbial degradation products influence colon cancer risk: the butyrate controversy. *J Nutr* 2004;134:479–82.
46 Putaala H, Mäkivuokko H, Tiihonen K, *et al*. Simulated colon fiber metabolome regulates genes involved in cell cycle, apoptosis, and energy metabolism in human colon cancer cells. *Mol Cell Biochem* 2011;357:235–45.
47 Chuah L-O, Foo HL, Loh TC, *et al*. Postbiotic metabolites produced by Lactobacillus plantarum strains exert selective cytotoxicity effects on cancer cells. *BMC Complement Altern Med* 2019;19:114.